

# Direct Numerical Simulation of Supersonic Turbulent Boundary Layer Flow \*

GAO Hui(高慧)\*\*, FU De-Xun(傅德薰), MA Yan-Wen(马延文), LI Xin-Liang(李新亮)

State Key Laboratory of Nonlinear Mechanics, Institute of Mechanics, Chinese Academy of Sciences, Beijing 100080

(Received 7 January 2005)

*Direct numerical simulations of a spatially evolving supersonic flat-plate turbulent boundary layer flow with free Mach number  $M_\infty = 2.25$  and Reynolds number  $Re = 365000/in$  are performed. The transition process from laminar to turbulent flow is obtained by solving the three-dimensional compressible Navier–Stokes equations, using high-order accurate difference schemes. The obtained statistical results agree well with the experimental and theoretical data. From the numerical results it can be seen that the transition process under the considered conditions is the process which skips the Tollmien–Schlichting instability and the second instability through the instability of high gradient shear layer and becomes of laminar flow breakdown. This means that the transition process is a bypass-type transition process. The spanwise asymmetry of the disturbance locally upstream imposed is important to induce the bypass-type transition. Furthermore, with increasing the time disturbance frequency the transition will delay. When the time disturbance frequency is large enough, the transition will disappear.*

PACS: 47.27.Cn, 47.27.Nz

Turbulent flows can be found widely in nature and engineering applications. Physical understanding of the compressible wall turbulence is helpful to solve a lot of practical flows. Compressible flat-plate turbulent boundary layer flow is a typical and simple sample of wall turbulence for studying mechanisms of turbulence.

There have been relatively few attempts on direct numerical simulations (DNSs) of compressible spatially evolving flat-plate boundary layer flow transition and turbulence due to difficulties in both numerical simulation and experiment research. In order to minimize the computational resources for simulations, some CFD workers used the so-called temporal direct numerical simulation (TDNS) approach.<sup>[1–3]</sup> However, the quasi-periodic simulations used in the TDNS can bring model errors. Recently, a few DNSs for the spatially evolving flat-plate boundary layer flow have been performed. Rai *et al.*<sup>[4]</sup> and Pirozzoli *et al.*<sup>[5]</sup> performed the DNSs of spatially evolving adiabatic flat-plate boundary layer flows with Mach number  $M_\infty = 2.25$ . The emphasis of their studies is on assessment of validity of Morkovin's hypothesis, and the obtained results showed that the compressible turbulence with  $M_\infty = 2.25$  exhibits the feature close to the incompressible case. However, the transition process in the boundary layer flow has not been analysed in Refs. [4,5]. Meng *et al.*<sup>[6]</sup> analysed the transition process in a flat-plate boundary layer flow with a low Mach number  $Ma = 0.02$ .

In this Letter, a DNS of a spatially evolving compressible flat-plate boundary layer flow with  $M_\infty = 2.25$  and  $Re = 635000/in$  is performed. The same free flow conditions as used by Rai *et al.*<sup>[4]</sup> and Pirozzoli

*et al.*<sup>[5]</sup> are adopted. Based on numerical results, the transition characteristics are discussed.

In order to reach high resolution and high efficiency for solving the three-dimensional Navier–Stokes equations, high-order accurate methods are needed.<sup>[7–11]</sup> Here a seventh-order accurate upwind difference scheme for the convective terms, a sixth-order accurate central difference scheme for the viscous terms, and a three-step Runge–Kutta method for time discretization are used.<sup>[12]</sup> The three-dimensional computational domain consists of  $4.0\text{ in} \leq x \leq 9.6\text{ in}$  in the streamwise direction;  $0 \leq y \leq 0.2\text{ in}$  in the wall normal direction, and  $0 \leq z \leq 0.35\text{ in}$  in the spanwise direction. The total number of grid points is  $1280 \times 53 \times 240$  ( $x \times y \times z$ ).

In order to realize the inflow boundary and initial conditions for the three-dimensional computation, a DNS of a two-dimensional laminar compressible flat-plate boundary layer flow including the leading-edge is carried out. The computed two-dimensional results at  $x = 4.0\text{ in}$  are used as the inflow boundary conditions for the three-dimensional computation. The inflow boundary conditions used at present are different from those used in Refs. [4,5]. The treatment of inflow boundary conditions in our computation can avoid the inconsistency due to the commonly adopted experiential formulae which do not satisfy the Navier–Stokes equations. The normal upper boundary is located far from the plate and the non-reflecting boundary conditions can be used well. Usually the downstream boundary conditions influence greatly the results. Downstream non-reflecting treatment in our case gives satisfactory results. The non-slip conditions and constant temperature  $T = T_w$  are used on the

\* Supported by the National Natural Science Foundation of China under Grant Nos 10135013 and 90205025, and the Knowledge Innovation Project of Chinese Academy of Sciences under Grant No INF105-SCE.

\*\* Email: gaohui66@sohu.com

©2005 Chinese Physical Society and IOP Publishing Ltd

wall. In order to accelerate the transition process, a periodic-blowing suction disturbance on the upstream local wall ( $4.5 \text{ in} \leq x \leq 5.0 \text{ in}$ ) is introduced.<sup>[4]</sup> Here the normal velocity component is defined as

$$v_{bs} = Af(x)g(z)h(t), \quad (1)$$

$$f(x) = 4 \sin(\theta)[1 - \cos(\theta)]/(27)^{1/2}, \quad (2)$$

$$g(z) = \sum_{l=0}^{l_{\max}} Z_l \sin[2\pi l(z/z_{\max} + \phi_l)], \quad (3)$$

$$h(t) = \sum_{m=1}^{m_{\max}} T_m \sin[2\pi m(\beta t + \phi_m)]. \quad (4)$$

In the computation we take  $A = 0.04$ ,  $l_{\max} = 10$ ,  $m_{\max} = 5$ ,  $x_a = 4.5 \text{ in}$ ,  $x_b = 5.0 \text{ in}$ ,  $\beta = 2.5$  and the phase difference  $\phi_l$  and  $\phi_m$  as random numbers ranging from 0.0 to 1.0. Periodic conditions are imposed on the spanwise boundaries.

Some turbulence statistics results are presented and compared with the experimental data for validation. The turbulence statistics begins at  $t = 8.1$  and the total time samples are 50000.

The turbulence development for the spatially evolving flat-plate boundary layer flow can be judged by the distribution of energy spectra along the streamwise direction. Figure 1 gives the energy spectra for different wave numbers at  $y^+ = 1.03$  along the streamwise direction. It can be seen that the energy spectrum rises up in the disturbance region  $4.5 \text{ in} < x < 5 \text{ in}$  owing to the periodic blowing and suction disturbance. However, the high wave number spectra are still low and the energy difference between the spectra of the maximum and minimum wave numbers is about in two orders of magnitude (the logarithm scheme is adopted in Fig.1). Then the energy spectra with higher wave numbers are excited. This means that the transition starts in the boundary layer flow. In the region of  $x > 8.0 \text{ in}$ , the full developed turbulence with energy spectra of wide range wave numbers in the boundary layer flow is formed. Figure 2 shows the distribution of the computed skin-friction along the streamwise direction. The skin-friction rises up quickly when the boundary layer transition begins at about  $x > 6.2 \text{ in}$  and reaches its maximum at about  $x = 7.8 \text{ in}$ , then the skin-friction gradually approaches the turbulent value as the boundary layer flow develops into full turbulence. Figure 2 also shows fine agreement between the computational results and the results obtained from related theoretical relations.<sup>[5]</sup>

Figure 3 shows the computed mean velocity profile normalized by the wall-shear velocity at  $x = 8.8 \text{ in}$ . It can be seen that the computed results (solid line) are in good agreement with the combination of the wall law and the logarithm law. Figure 4 shows the turbulent intensity profiles normalized by the local mean velocity at  $x = 8.8 \text{ in}$ . The experimental data for in-

compressible flow<sup>[8]</sup> are also presented as the symbols in Fig. 4. It can be seen that the computed results agree well with the experimental data. The contours of density in the  $(x, y)$  plane at  $z = 0.044 \text{ in}$ ,  $8.5 \text{ in} \leq x \leq 9.5 \text{ in}$  are given in Fig. 5 from which the “burst” phenomenon can be seen clearly. That is, the fluids with lower density inject upward from the wall region and the fluids with higher density sweep down. The above discussions show that obtained DNS results are valid for the spatially evolving supersonic flat-plate boundary layer flow from laminar through transition to turbulence, and Morkovin’s hypothesis is tenable owing to the low free Mach number of 2.25.

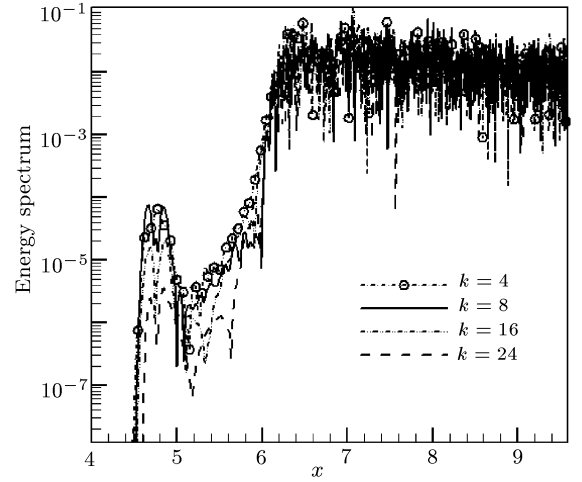


Fig. 1. Energy spectra in versus  $x$  at  $y^+ = 1.03$  for different wave numbers.

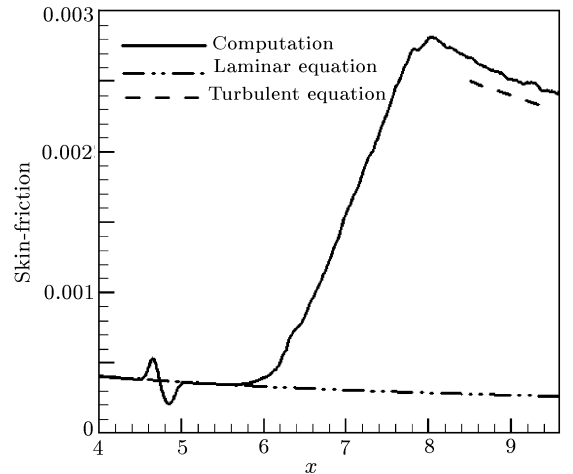
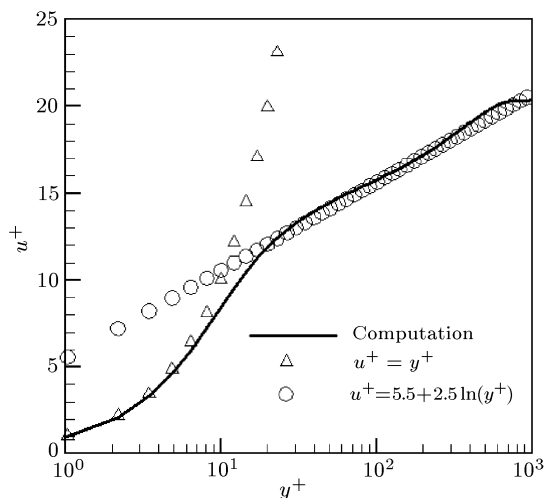


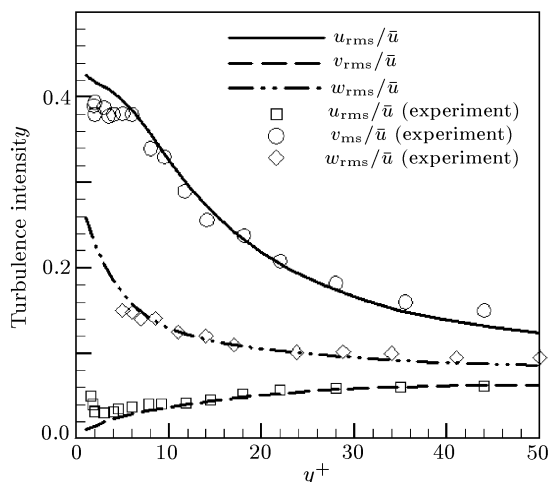
Fig. 2. Skin-friction along the flat-plate.

Figure 6 shows the contours of the streamwise vorticity in the  $(x, y)$  plane at different times ( $y^+ = 1.03$ ). It can be seen that the streamwise vorticity first appears in the disturbance region,  $4.5 \text{ in} < x < 5.0 \text{ in}$ , then the streamwise vorticity appears one the one side of the spanwise direction due to spanwise asymmetry

of imposed disturbance in this region, later it appears on the other side. In the development of the boundary layer flow the vortex merge in the spanwise direction is produced.



**Fig. 3.** Mean velocity profile normalized by wall shear velocity ( $x = 8.8$  in.).



**Fig. 4.** Turbulence intensities normalized by local mean velocity at  $x = 8.8$  in.

Meanwhile, it can be seen that after the disturbance region, a high gradient shear layer appears at  $t = 3.75$  (near  $x \approx 7.0$  in, see Fig. 7), and a pair of counter-rotating streamwise vortices which can be seen from the streamwise vorticity contours in  $(x, y)$  plane are formed. Then the high gradient shear layers move to downstream and become unstable in the transition region (see Fig. 7,  $t = 5.88$ ). The instability of this high-shear layer leads to laminar breakdown. Finally, a fully developed turbulent boundary layer flow is formed in the region  $x > 8$  in. (see Fig. 6,  $t = 8.66$  and Fig. 7,  $t = 8.2$ ). The  $\Lambda$  vortex is not found in the numerical results.

The above transition description shows that the

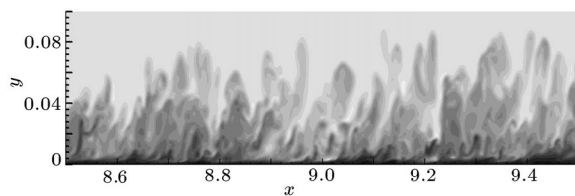


**Fig. 5.** Contours of density in the  $(x, y)$  plane  $z = 0.044$  in.

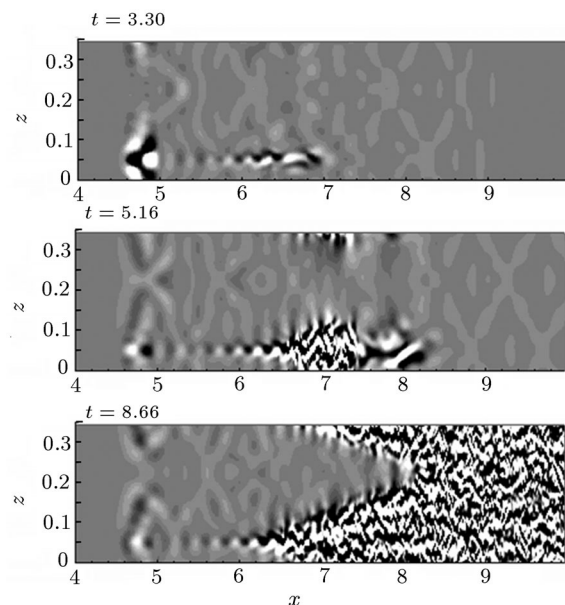


**Fig. 6.** Contours of the streamwise vorticity  $\omega_x$  in the plane  $(x, z)$  at  $y^+ = 1.03$ .

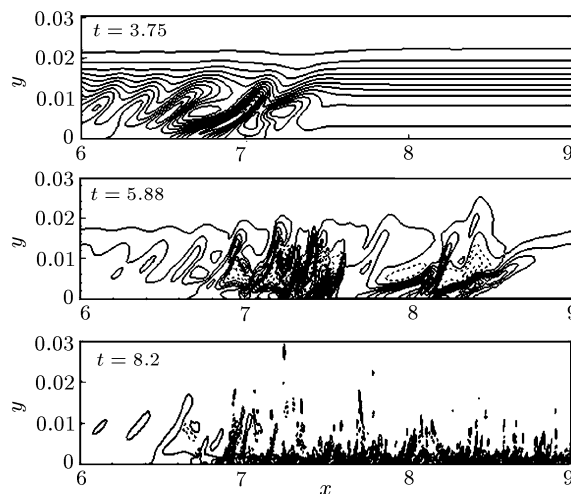


**Fig. 7.** Contours of the spanwise vorticity on the  $(x, y)$  plane at  $z = 0.018$  in at different times.

spanwise asymmetry of the imposed disturbance accelerates the transition process. It can be seen that the transition process of the flow under the present conditions is the process which skips the

Tollmien–Schlichting instability and the second instability through the instability of the high gradient shear layer and goes to laminar breakdown. This means that the transition process is a bypass-type transition process.

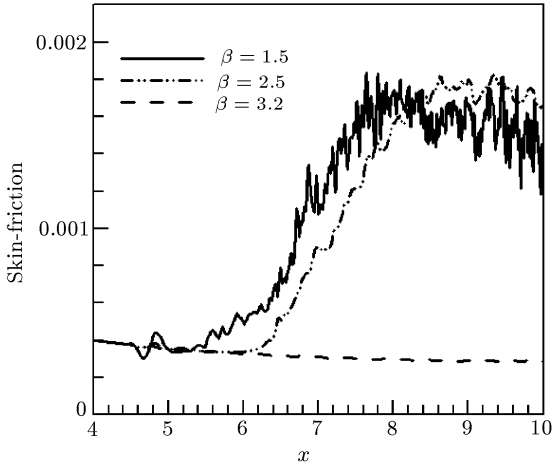


Fig. 8. Skin friction for  $\beta = 1.5, 2.5, 3.2$ .

From numerical results it can be seen that the time disturbance frequency  $\beta$  in Eq. (4) has also an influence on the boundary layer flow transition process. Three cases for  $\beta = 3.2, 1.5, 2.5$  are computed for testing the  $\beta$  influence, under the same computational conditions that the three-dimensional computational domain consists of  $4.0\text{ in} \leq x \leq 10.0\text{ in}$ ,  $0 \leq y \leq 0.2\text{ in}$ ,  $0 \leq z \leq 0.35\text{ in}$ , and the total number of grid points is  $768 \times 128 \times 64$  ( $x \times y \times z$ ). Figure 8 shows the skin-friction along the streamwise direction for  $\beta = 3.2, 1.5$  and  $2.5$ . It can be seen that the skin-friction reduces continually in the streamwise direction and tends to a laminar value for the case  $\beta = 3.2$ . This means that the transition process does not appear in the flow for the case of  $\beta = 3.2$ . However, in the boundary layer, the flow transition process appears for the lower time disturbance frequency  $\beta = 1.5$  and  $2.5$ . In comparison of the skin-friction between the cases  $\beta = 1.5$  and  $2.5$ , it can be seen that for the lower time disturbance frequency  $\beta = 1.5$  the boundary layer flow transition

starts at  $x = 5.4\text{ in}$ , but transition starts at  $x = 6.2\text{ in}$  for the case of  $\beta = 2.5$ . It can be concluded that in the region of the time disturbance frequency which can induce the turbulence, the transition can be delayed with the increasing time frequency.

Direct numerical simulation for a spatially evolving supersonic flat-plate boundary layer flow from the laminar through transition process to full developed turbulence with  $M_\infty = 2.25$  has been carried out. The transition process of the flow under the present condition is a skipping process over the Tollmien–Schlichting instability and the second instability and it is a bypass-type transition. The instability of the high gradient shear layer in the boundary layer flow and the spanwise asymmetry of the imposed disturbance play an important role in the bypass transition process.

The transition can be put off with the higher time frequency in the region of the time frequency which can induce the turbulence.

## References

- [1] Guo Y and Adams N A 1994 *Proc. 1994 Summer Program of the Center for Turbulence Research* (California: Stanford University) p 245
- [2] Guarini S E, Moser R D, Shariff K and Wray A 2000 *J. Fluid Mech.* **414** 1
- [3] Maeder T, Adams N A and Kleiser L 2001 *J. Fluid Mech.* **429** 187
- [4] Rai M M, Gatski T B and Erlebacher G 1995 *AIAA* **95** 0583
- [5] Pirozzoli S, Grasso F and Gatski T B 2004 *Phys. Fluids* **16** 530
- [6] Meng W, Sanjiva K L and Parviz M 1996 *J. Fluid Mech.* **319** 197
- [7] Tian B L, Fu D X and Ma Y W 2004 *Chin. Phys. Lett.* **21** 1770
- [8] Fu S, Li Q B and Wang M H 2003 *Chin. Phys. Lett.* **20** 2193
- [9] Wang B, Zhang H Q and Wang X L 2004 *Chin. Phys. Lett.* **21** 1773
- [10] Liu W and Jiang N 2004 *Chin. Phys. Lett.* **21** 1989
- [11] Liu S, Zhou B H, Nguyen T H and Hu W R 2004 *Chin. Phys. Lett.* **21** 686
- [12] Fu D X and Ma Y W 2002 *Computational Fluid Dynamics* (Beijing: Higher Education Press) p 85 (in Chinese)